Frontiers in Bioscience Landmark

Front. Biosci. (Landmark Ed) **2026**; 31(7): 51862
https://doi.org/10.31083/FBL51862

Original Research

Troxerutin Activity Against Oxidative Stress: A Potential Strategy for Corneal Damage Evaluated in a 3D Model of Human Corneal Epithelial Cells

Rossella Basilotta[1,†], Alessia Filippone[2,†], Nicoletta Palermo[3], Giovanna Casili[1], Marika Lanza[1], Emanuela Esposito[1,*], Irene Paterniti[1]

[1]Department of Chemical, Biological, Pharmaceutical and Environmental Sciences, University of Messina, 98166 Messina, Italy
[2]Department of Medicine and Surgery, UniCamillus-Saint Camillus International University of Health Sciences, 00131 Rome, Italy
[3]Department of Biochemical, Dental, Morphological and Functional Imaging, University of Messina, 98125 Messina, Italy
*Correspondence: emanuela.esposito@unime.it (Emanuela Esposito)
[†]These authors contributed equally.

Academic Editor: Sarah D. Atkinson
Submitted: 13 March 2026 Revised: 17 June 2026 Accepted: 30 June 2026 Published: 27 July 2026

Abstract

Background: Oxidative stress and inflammation are closely associated with ocular surface disorders, including dry eye disease (DED), keratitis, and corneal erosion. These pathological processes contribute to an imbalance in tear composition and induce structural and functional alterations of the cornea. In this context, natural compounds with antioxidant and anti-inflammatory activities have emerged as promising strategies for preserving ocular health and mitigating the effects of corneal injuries. In the present study, we investigated the potential protective effects of troxerutin (TX), a naturally occurring flavonoid, in attenuating oxidative stress and promoting the restoration of corneal tissue architecture. **Methods:** To this end, an H_2O_2-induced oxidative stress model was established using human corneal epithelial cells (HCE) SkinEthic™ 3D tissues. Cells were pretreated with TX and, after 24 hours, stimulated with H_2O_2 for 10 minutes. **Results:** TX showed a protective effect against oxidative injury in the HCE 3D model and supported morphological recovery consistent with re-epithelialization through the upregulation of tight junction proteins zona occludens-1 (*ZO-1*) and *Occludin*. In addition, TX helped attenuate inflammatory responses by regulating interleukin-6 (*IL-6*), interleukin-8 (*IL-8*), matrix metallopeptidase 9 (*MMP-9*), and key adhesion molecules, including intercellular adhesion molecule-1 (*ICAM-1*) and *P-selectin*. **Conclusions:** Overall, these findings emphasize the potential of TX as a natural compound that may contribute to the prevention and management of corneal damage.

Keywords: corneal injuries; dry eye syndromes; oxidative stress; tight junction proteins; inflammation

1. Introduction

The corneal epithelium serves as a critical barrier against various forms of injury, trauma, and infection, playing a key role in shielding the eye from UV radiation, harmful pollutants, and physical damage [1,2,3,4]. The ocular surface, in fact, is continuously exposed to oxidative factors such as environmental oxygen, photooxidation, ionizing radiation, cigarette smoke, and environmental pollutants. Oxidative stress can impact all cellular components, altering enzyme activity, inhibiting nucleic acid and protein synthesis, and upregulating proinflammatory gene expression, thereby triggering inflammation [5]. The ocular surface is vulnerable to oxidative imbalance, being widely exposed to light and extensive metabolic activity. Excessive intracellular accumulation of reactive oxygen species (ROS) can therefore lead to lipid peroxidation of membranes, protein modification, and DNA damage, resulting in ocular surface homeostasis dysfunction [6]. Among the most common oxidative stress-related conditions is dry eye disease (DED), a multifactorial disorder. This condition manifests with debilitating symptoms such as foreign body sensation, redness, burning, eye fatigue, and visual disturbances, significantly impacting patients' quality of life [7,8]. Several studies reported increased oxidative stress in the tears and conjunctiva of patients with DED, caused by frequent sources of ROS production [9,10,11] with elevated levels of some oxidizing enzymes such as myeloperoxidase (MPO), nitric oxide synthase (NOS2, NOS3) and xanthine oxidase/oxidoreductase and high levels of lipid peroxidation products such as lipid peroxide (LPO), hexanoyl-lysine (HEL), 4-hydroxy-2-nonenal (4-HNE), and malondialdehyde (MDA) [12,13]. Other oxidative stress-induced corneal disorders include neurotrophic keratitis, a condition marked by corneal sensitivity loss which is often worsened by oxidative stress and uncontrolled inflammation [2,14]. While current therapies focus on targeting inflammation, recent findings suggest that exclusively inhibiting inflammation may not be sufficient for treating these multifactorial and chronic conditions [15]. This limitation arises from the involvement of an upstream mediator, i.e., the excessive production of ROS, which can compromise therapeutic efficacy [16,17]. In recent years, natural compounds with antioxidant prop-

erties have gained increasing attention as potential protective agents against oxidative damage to the cornea. Among these, esculetin (6, 7-dihydroxycoumarin) played an antioxidant role enhancing nuclear factor erythroid 2-related factor 2 (Nrf2) signaling and regulating antioxidant genes like Heme oxygenase-1 (*HO-1*), NAD(P)H Quinone Dehydrogenase (*NQO1*), Glutamate-Cysteine Ligase Modifier Subunit (*GCLM*), Superoxide Dismutase type 1 and 2 (*SOD1* and *SOD2*) mRNA expression levels in H_2O_2-treated human corneal epithelial cells (HCE) [18]. Likewise pterostilbene (PS), a natural component of blueberries, protected the cornea from inflammation and hyperosmolarity induced by oxidative stress, reducing the expression of pro-inflammatory mediators, tumor necrosis factor alpha (*TNF-α*), interleukin-1 beta (*IL-1β*), interleukin-6 (*IL-6*), matrix metallopeptidase 2 and 9 (*MMP-2* and *MMP-9*) and markers of oxidative damage, *MDA*, *4-HNE* and 8-Hydroxy-deoxyguanosine (*8-OHdG*) [19]. Lately, troxerutin (TX), a flavonoid derived from rutin, commonly known as vitamin P4 [20] has sparked pharmacological interest for its antioxidant properties and potential health benefits in different tissues, e.g., liver, kidney and brain [21,22,23,24] by counteracting various conditions, including, neurodegenerative disorders, cardiovascular diseases, metabolic syndromes, renal protection, and cancer-related oxidative damage [20,25,26,27,28,29,30]. More recent evidence has highlighted its relevance in vascular and microvascular homeostasis, with particular interest in ocular tissues. In this context, troxerutin has been reported to counteract hyperglycemia-induced vascular endothelial growth factor (*VEGF*) upregulation in endothelial cells, suggesting a protective role in the early stages of diabetic retinopathy and retinal microvascular dysfunction [31,32]. The aim of this study was to test the potential protective effect of TX in a 3D model of corneal tissue to explore a novel therapeutic approach for oxidative stress-related corneal disorders.

2. Materials and Methods

2.1 Materials

Troxerutin (TX) was acquired from Sigma-Aldrich Corporation (Cat. # PHR2815). TX and all stock solutions were dissolved in basal medium.

2.2 SkinEthic™ HCE Model

The SkinEthic™ HCE model was obtained from EPISKIN Laboratories (Nice, France, EU). These human corneal epithelial cells were used as an *in vitro* system based on transformed corneal keratinocytes cultured on an inert polycarbonate membrane. This model closely mimics the structure, morphology, and function of the human cornea, including the presence of basal and wing cell layers as well as mucus production. SkinEthic™ HCE cells are derived from an immortalized human corneal epithelial cell line, not directly from limbal epithelial stem cells or other types of stem cells. These cells are typically used to reconstruct a three-dimensional, stratified, non-keratinized corneal epithelium model, which mimics the *in vivo* human corneal epithelium. The immortalization allows for consistent, reproducible results in toxicology and ophthalmic research. Therefore, the SkinEthic™ HCE model represents a valid and practical tool for exploring the cellular and molecular effects of oxidative damage on the corneal epithelium, suitable for studying direct epithelial responses to various stimuli, including oxidative stress, and for screening protective or therapeutic compounds. SkinEthic™ HCE tissues were grown on 0.5 cm^2 polycarbonate membrane inserts under air–liquid interface conditions in a chemically defined culture medium [33]. The inserts carrying the epithelial cultures were shipped in multiwell plates containing an agarose-enriched nutrient matrix used to maintain tissue integrity during transport. The human corneal epithelial tissue cultures were carefully removed from the agarose matrix and placed into 24-well plates containing 300 µL of fresh maintenance medium per well. HCE cell lines were validated by STR profiling. After confirming that no air bubbles were present beneath the culture inserts, the tissues were incubated overnight at 37 °C with 5% CO_2 and were mycoplasma-free (InvivoGen rep-mys-10). Following the equilibration step, the cultures were transferred to new 24-well plates containing 300 µL of SkinEthic maintenance medium for subsequent treatments [34].

2.3 In Vitro Model of Oxidative Stress by Using H_2O_2

Triplicate *in vitro* tissues were pre-treated with TX for 24 hours. Troxerutin (TX) was dissolved in culture medium and further diluted to reach the final working concentrations used in the experiments (30 and 50 µM). The same solvent was used as vehicle control in all corresponding experimental conditions. Hydrogen peroxide (H_2O_2) was freshly prepared by diluting the stock solution in culture medium immediately before use to achieve the final concentration of 200 µM [35]. After 24 hours *in vitro*, tissues were stimulated with H_2O_2 200 µM (H1009, Sigma-Aldrich) for 10 minutes, as previously described [36], to determine the oxidant effect. HCE were plated and treated as follows:

- CTR: HCE control cells grown in normal culture medium for 24 h (negative control).

- H_2O_2: HCE were stimulated with H_2O_2 (200 µM) for 10 min (positive control).

- H_2O_2 + TX 30 µM: HCE were pre-treated with TX at the concentration of 30 µM for 24 h and H_2O_2 200 µM for 10 min.

- H_2O_2 + TX 50 µM: HCE were pre-treated with TX at the concentration of 50 µM for 24 h and H_2O_2 200 µM for 10 min.

2.4 Hematoxylin and Eosin Assay

HCE tissues were fixed in 10% buffered formalin for 24 h at room temperature. Samples were subsequently

dehydrated through a graded ethanol series and xylene before paraffin embedding. Paraffin blocks were sectioned into 7 µm slices and stained with hematoxylin and eosin (H&E). Histological evaluation was performed using a Nikon Eclipse Ci-L microscope. Representative images were acquired at 20× magnification (20 µm scale bar). All histopathological evaluations were conducted under blinded conditions [37]. Overall tissue morphology and related alterations were evaluated in comparison with untreated controls using predefined histological criteria. These parameters included the number of epithelial layers, cellular morphology and distribution (flattened migrating cells versus cuboidal post-migratory cells), the presence of condensed nuclei associated with re-epithelialization, extracellular matrix (ECM) organization and staining characteristics, tissue compactness, and the integrity of cell–cell as well as cell–matrix interactions. For each parameter, a score from 1 to 4 was assigned to quantify the degree of tissue organization and recovery. Specifically, histological scores were assigned according to the degree of tissue preservation and recovery, where score 1 indicated normal histological appearance comparable to untreated controls, with preserved epithelial organization, compact tissue structure, and intact cell–cell and cell–matrix interactions; score 2 indicated mild morphological alterations with largely preserved tissue architecture; score 3 indicated moderate tissue damage and partial tissue disorganization; and score 4 indicated severe epithelial disruption, marked extracellular matrix alterations, and loss of tissue compactness. Evaluations were independently conducted by three experienced observers under blinded conditions, taking inter-rater reliability into consideration.

2.5 Cell Viability Assay

Following treatments, tissues were carefully rinsed with saline phosphate buffer and transferred to a freshly prepared MTT (3-(4,5-dimethylthiazol-2-yl)-2,5-diphenyltetrazolium bromide) solution (0.5 mg/mL in maintenance medium; 300 µL) in 24-well plates. The plates were then incubated for 3 h ± 15 min at 37 °C with 5% CO_2. After incubation, HCE tissues were removed from the MTT solution and transferred to a new 24-well plate containing 750 µL of isopropanol per well to solubilize the reduced MTT (formazan crystals). An additional 750 µL of isopropanol was added onto each tissue, and the plate was sealed with parafilm to prevent evaporation. Plates were gently shaken for at least 90 min at room temperature to ensure complete extraction of the formazan crystals. Subsequently, three 200 µL aliquots of the extracted solution were transferred to a flat-bottom 96-well plate, and optical density (OD) was measured at 570 ± 30 nm using a microplate reader [38].

The percentage viability of each of the treated cultures was calculated from the percentage MTT conversion in the test chemical treated cultures relative to the corresponding negative controls. Results were expressed as a percentage of viability compared to the negative control.

$$\% \text{ Viability} = [\text{OD test compound} \,/\, \text{OD negative control}] \times 100$$

2.6 WB Analysis for Oxidative Stress Antibody Detection

Western blot analysis was executed on protein extracted from SkinEthic™ HCE cells as previously described [39]. Briefly, all samples were resuspended in lysis buffer containing 20 mM Tris-HCl pH 7.5, 10 mM NaF, 150 µL of NaCl 5M, 1% Nonidet P-40 and protease cocktail of inhibitors (Catalog No. 11836153001; Roche, Switzerland) and after 40 minutes, lysates were centrifuged at 12,000 rpm for 15 minutes at 4 °C. Protein concentration was determined in the cleared lysates using the Bio-Rad protein assay with bovine serum albumin (BSA) as the calibration standard. Samples were denatured at 95 °C for 5 min, and equal amounts of protein were resolved on 12% SDS–PAGE gels before transfer onto PVDF membranes (Immobilon-P). Membranes were incubated overnight at 4 °C with primary antibodies against *SOD* (1:500, sc-137254, Santa Cruz, Dallas, TX, USA) or *HO-1* (1:500, Cat# SPA-895, StressGen-6055, San Diego, CA, USA), *IL-6* (1:500, 66146-1, Proteintech-Segrate (MI), Italy), *IL-8* (1:500, 109-401-311-0100, Thermofisher, Segrate (MI), Italy), *IL-1β* (1:500, ab254360, Abcam, Cambridge Biomedical Campus, Cambridge, UK), nuclear factor kappa B (NF-κB) (1:500, sc-372, Santa Cruz, Dallas, TX, USA), *MMP-9* (1:500, sc-393859, Santa Cruz, Dallas, TX, USA). To verify equal protein loading, membranes were additionally probed with an anti-β-actin antibody (1:1000, sc-47778, Santa Cruz, Dallas, TX, USA).

2.7 Measurement of NO_2^- Levels in HCE Cell Supernatant

Nitrite levels, used as an indirect marker of *nitric oxide* (*NO*) production, were quantified in the supernatants of pretreated HCE cells [40]. Briefly, nitrate present in the medium was converted into nitrite through incubation with nitrate reductase (670 mU/mL) and β-nicotinamide adenine dinucleotide phosphate (160 mM) at room temperature for 3 h. Total nitrite levels, as an indicator of NO production, were subsequently determined using the Griess reaction by mixing 100 µL of sample with 100 µL of Griess reagent, consisting of 0.1% (w/v) N-(1-naphthyl)ethylenediamine dihydrochloride in water and 1% (w/v) sulfanilamide in 5% (v/v) concentrated H_3PO_4 (1:1, v/v). Absorbance was measured at 570 nm. Nitrite (NO_2^-) levels, as an indicator of NO production, were assessed exclusively at the 24 h time point, corresponding to the longer exposure condition, based on the cell viability findings.

2.8 Enzyme-Linked Immunosorbent Assay (ELISA Kit) for Catalase (CAT) and Nrf2

ELISA kits for CAT (Human Catalase cat.n. RK09250 ABclonal) and Nrf2 (Human Nrf2 ELISA kit A7064, antibodies) were used according to the manufacturer's in-

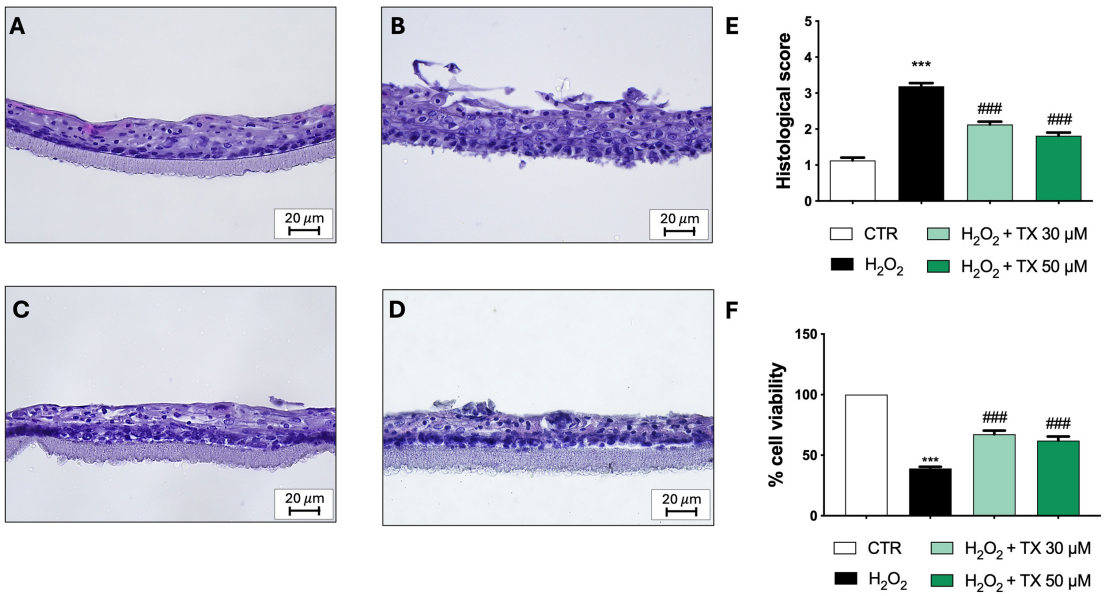

Fig. 1. Effect of troxerutin on HCE tissue morphology. H&E staining showed tissue disorganization and irregular cell-cell contacts in the H_2O_2 group compared to CTR, while TX treatment (30 and 50 µM) improved tissue architecture and corneal surface regularity. (A) CTR group. (B) H_2O_2 Group. (C) H_2O_2 Group + TX 30 µM Group. (D) H_2O_2 Group + TX 50 µM Group. (E) Histological score. (F) Cell viability assay on HCE tissues. Values are means ± SEM. *** $p < 0.001$ vs group CTR; ### $p < 0.001$ vs H_2O_2 group. One-way ANOVA test followed by Bonferroni post hoc test for multiple comparisons was used. HCE, human corneal epithelial cells; H&E, hematoxylin and eosin; H_2O_2, hydrogen peroxide; CTR, control group; TX, troxerutin; SEM, standard error of the mean; ANOVA, analysis of variance. Scale bar: 20 µm.

structions. Cell culture supernatants or lysates were centrifuged at 3000 rpm for 10 min, after which the clarified supernatants were used for immediate analysis. Absorbance readings were recorded at 450 nm.

2.9 Immunohistochemistry Assay for Tight Junctions and Adhesion Molecules

Immunohistochemical localization for *ICAM-1* (intercellular adhesion molecule-1, 1:100; sc-7891, Santa Cruz), *P-selectin* (1:100; sc-6941, Santa Cruz), zona occludens-1 (*ZO-1*) antibodies (1:100; sc-33725, Santa Cruz), and *Occludin* (1:100; sc-133256, Santa Cruz) was conducted as previously described [41]. Briefly, tissue sections were incubated overnight with the primary antibodies, washed with PBS, and subsequently exposed to the appropriate secondary antibody for 1 h. Immunoreactivity was visualized using the water-soluble chromogenic substrate 3,3′-diaminobenzidine (DAB), followed by counterstaining with Nuclear Fast Red. The immunopositive area, calculated as the percentage of positive pixels relative to the total tissue area, was quantified in five randomly selected fields using a 40× objective and analyzed with a computerized image analysis system (Leica QWin V3, Cambridge, UK). Representative images were acquired at 20× magnification using a Nikon Eclipse Ci-L microscope. Staining intensity was quantified according to a semi-quantitative scale ranging from 0 to 10, where 0 corresponded to the absence of brown immunoreactivity, and 10 indicated intense dark-brown staining. Evaluations were independently conducted by three experienced observers under blinded conditions.

2.10 Statistical Analysis

Data are expressed as mean ± standard error of the mean (SEM) from three independent biological experiments. Each experimental condition was analyzed using technical replicates, as specified in the corresponding assay descriptions. Statistical analysis was performed using GraphPad Prism 9.5.1 software (Boston, MA, USA). Differences among groups were evaluated by one-way analysis of variance (ANOVA), followed by Bonferroni's multiple comparison test. Differences were considered statistically significant at $p \leq 0.05$.

3. Results

3.1 Troxerutin Remodeled HCE Tissue Architecture From H_2O_2-Induced Oxidative Damage

Tissue morphology was assessed by H&E staining to investigate the changes in HCE tissue structure, following the induction of oxidative stress by H_2O_2, analyzing the morphological factors involved in re-epithelialization and remodeling [37]. Morphological analysis by H&E at 24 hours showed a disorganization of the tissue architecture, with irregular cell-cell contacts in the H_2O_2 group than in the control (Fig. 1A,B,E). TX treatment at concentrations of 30 µM and 50 µM, was able to protect against the induced

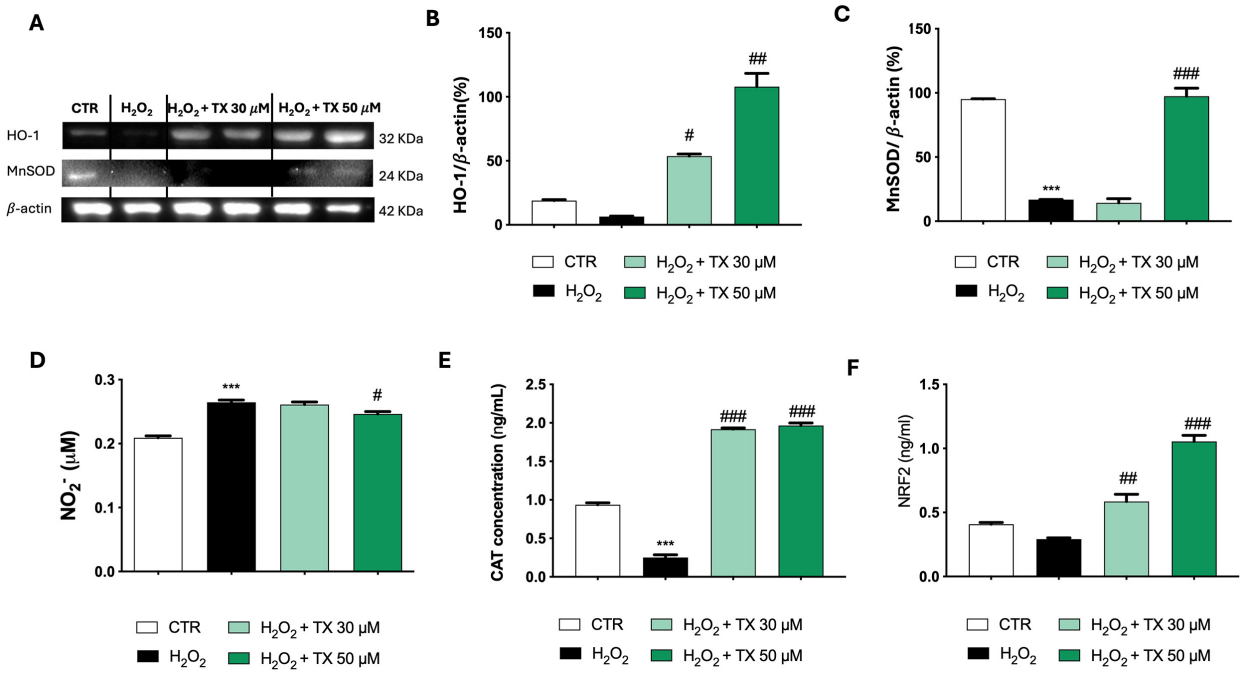

Fig. 2. Effect of troxerutin on H_2O_2-induced oxidative stress on HCE tissues. TX treatment increased the expression of the antioxidant enzymes *HO-1* and *MnSOD* and reduced H_2O_2-induced nitrite production, while enhancing *CAT* levels, supporting its protective antioxidant effect. (A) Western blot analysis for the evaluation of *HO-1* and *MnSOD* protein expression. (B) Quantification of *HO-1* expression. (C) Quantification of *MnSOD* expression. (D) Griess assay on HCE supernatants. (E) ELISA assay for the evaluation of *CAT* levels on HCE supernatants. (F) ELISA assay for the evaluation of *Nrf2* levels. Values are means ± SEM. *** $p < 0.001$ vs group CTR; # $p < 0.05$; ## $p < 0.01$; ### $p < 0.001$ vs H_2O_2 group. One-way ANOVA test followed by Bonferroni post hoc test for multiple comparisons was used. *Nrf2*, nuclear factor erythroid 2-related factor 2; *HO-1*, heme oxygenase-1; *MnSOD*, manganese superoxide dismutase; *CAT*, catalase.

injury by restoring the re-epithelialization processes, showing a more organized and regular morphological structure and a smoother corneal surface (Fig. 1C,D,E). The effect of TX treatment on HCE cell viability was assessed via MTT assay. Following H_2O_2 exposure, there was an observed decrease in HCE cell viability in comparison with untreated control cells. Cell viability in the TX-treated group at both concentrations of 30 and 50 µM increased significantly as compared to H_2O_2-treated cells (Fig. 1F).

3.2 Troxerutin Showed an Antioxidant Effect by Modulating Antioxidant Markers

The effect of TX in the modulation of antioxidant response was evaluated by western blot analysis, which revealed an increase in the expression of antioxidant enzymes *HO-1* and *MnSOD* following TX treatment, suggesting its protective role in enhancing the endogenous antioxidant system and mitigating H_2O_2-induced oxidative stress (Fig. 2A–C). In addition, the Griess assay was used to quantify nitrite levels in the supernatant of HCE tissues after treatment with hydrogen peroxide (H_2O_2) and TX. Since nitrite is a stable oxidation product of nitric oxide (NO), it was used as an indirect indicator of NO production. The results showed increased nitrite levels in tissues exposed to H_2O_2 compared to baseline control levels (Fig. 2D). Treatment with TX significantly reduced nitrite levels compared with H_2O_2 treatment alone, particularly at the concentration of 50 µM, suggesting its effectiveness in mitigating H_2O_2-induced oxidative stress and the associated increase in NO-derived reactive species, whereas no significant changes were observed following treatment with 30 µM TX (Fig. 2D). In line with these results, the ELISA assay showed a significant rise in antioxidant enzyme *CAT* levels in the supernatants collected following treatment with 30 µM and 50 µM TX when compared to the H_2O_2 group (Fig. 2E). Furthermore, to elucidate the upstream molecular mechanism driving this antioxidant response, the expression of nuclear factor erythroid 2-related factor 2 (Nrf2) was quantified using an ELISA kit. The results revealed a significant upregulation of Nrf2 levels in TX-treated groups compared to the H_2O_2-alone group, indicating that TX promotes the activation and nuclear translocation of Nrf2 to induce downstream antioxidant enzymes (Fig. 2F).

3.3 Troxerutin Reduced Cytokine Release and MMP-9 Expression

To further investigate the modulation of the inflammatory response induced by oxidative stress, the expression

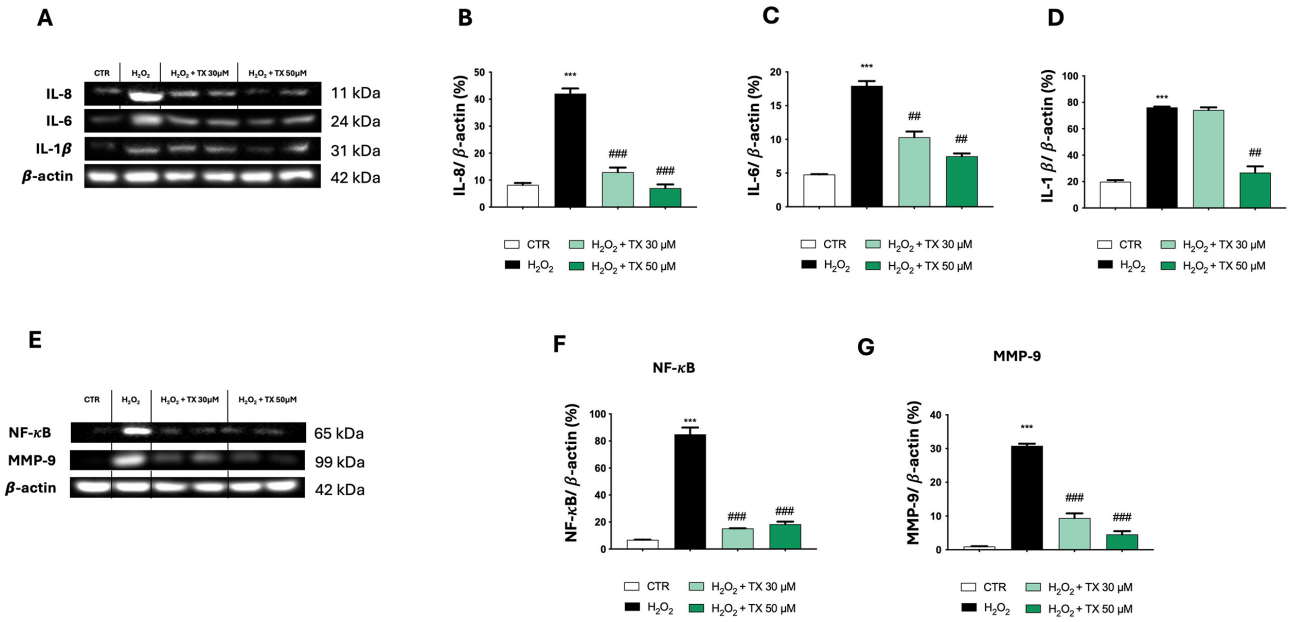

Fig. 3. Effect of TX on *IL-8*, *IL-6*, *IL-1β*, NF-κB and *MMP-9* expression in H_2O_2-stimulated HCE tissues. H_2O_2 treatment significantly increased the expression of the pro-inflammatory cytokines. Conversely, TX treatment (30 and 50 µM) significantly reduced the expression of all these inflammatory mediators. (A–D) Representative Western blot images for IL-8 (B), IL-6 (C), and IL-1β (D) and respective quantifications. (E–G) Representative Western blot images for NF-κB (F), and MMP-9 (G) and respective quantifications. Values are means ± SEM. *** $p < 0.001$ vs CTR group; ## $p < 0.01$; ### $p < 0.001$ vs H_2O_2 group. One-way ANOVA followed by Bonferroni post hoc test for multiple comparisons was used. *IL-8*, interleukin-8; *IL-6*, interleukin-6; *IL-1β*, interleukin-1 beta; NF-κB, nuclear factor kappa B; *MMP-9*, matrix metallopeptidase 9.

and release of the pro-inflammatory mediators IL-8, IL-6, IL-1β, and MMP-9 were evaluated in HCE tissues exposed to H_2O_2.

Western blot analyses revealed a significant increase in the levels of these inflammatory markers following H_2O_2 stimulation when compared to baseline control conditions, suggesting the activation of inflammatory pathways associated with oxidative damage (Fig. 3A–G). Treatment with TX reduced the expression and release of IL-8, IL-6, and IL-1β (Fig. 3A–D) and MMP-9 (Fig. 3G) compared with tissues treated with H_2O_2 alone, particularly at the concentration of 50 µM. To gain a deeper insight into the underlying molecular mechanisms and evaluate the upstream signaling cascade, we further investigated the key regulatory protein NF-κB. Exposure to H_2O_2 led to a marked upregulation of NF-κB (Fig. 3F), establishing a clear link between oxidative insult and the activation of the master inflammatory transcriptional pathway. Notably, treatment with TX effectively counteracted this effect, significantly reducing the protein expression levels of NF-κB back towards baseline conditions (Fig. 3F).

These results suggest that TX exerts a protective anti-inflammatory effect by strictly down-regulating the upstream NF-κB signaling axis, thereby regulating the downstream molecular pathways involved in cytokine production, preserving tissue integrity and limiting inflammation-associated damage.

3.4 Troxerutin Restored the Integrity of the Epithelial Barrier of HCE Tissues

ZO-1 and *Occludin* are key proteins that play a crucial role in preserving the protective function of the cornea against oxidative stress and environmental damage [42]. Our results show that HCE tissue exposed to H_2O_2-induced oxidative stress has a lower *ZO-1* and *Occludin* expression, revealing a significant impairment of epithelial barrier integrity compared to control (Fig. 4A,B for *ZO-1*; Fig. 4F,G for *Occludin*). Treatment with TX at concentrations of 30 µM and 50 µM was able to significantly increase the expression levels of these tight junctions compared to the H_2O_2 group (Fig. 4C–E for *ZO-1*; Fig. 4H–J for *Occludin*), suggesting a protective effect in restoring the integrity of the epithelial barrier.

3.5 Troxerutin Modulated the Integrity of the Epithelial Barrier of HCE Tissues

ICAM-1 and *P-selectin* expression was evaluated in the HCE 3D model to assess the anti-inflammatory effect of TX. Exposure to the inflammatory-oxidative stimulus as H_2O_2 resulted in a significant upregulation of both *ICAM* and *P-selectin* immunopositivity (Fig. 5B,G, respectively) compared with the untreated control group (Fig. 5A,F, respectively), indicating activation of epithelial cells and increased expression of adhesion molecules involved in inflammatory cell recruitment. Treatment with TX at both

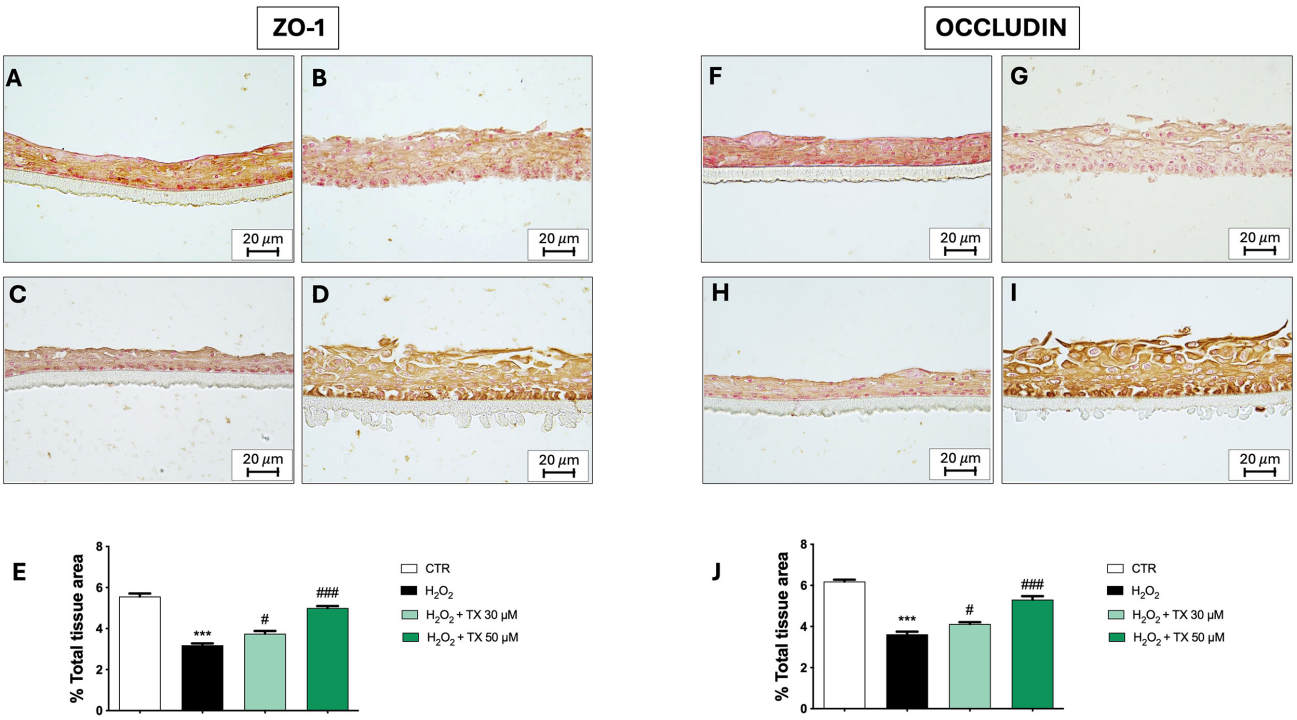

Fig. 4. Effect of troxerutin on *ZO-1* and *Occludin* immunopositivity. H_2O_2 treatment reduced the expression of *ZO-1* and *Occludin*, indicating impairment of epithelial barrier integrity, while TX treatment (30 and 50 µM) restored tight junction protein expression. (A,F) CTR group. (B,G) H_2O_2 Group. (C,H) H_2O_2 + TX 30 µM Group. (D,I) H_2O_2 + TX 50 µM Group. (E,J) The percentage of total tissue area. Values are means ± SEM. *** $p < 0.001$ vs group CTR; # $p < 0.05$; ### $p < 0.001$ vs H_2O_2 group. One-way ANOVA test followed by Bonferroni post hoc test for multiple comparisons was used. *ZO-1*, zona occludens-1. Scale bar: 20 µm.

concentrations significantly reduced the immunopositivity of both markers in the HCE 3D model (Fig. 5C,D,H,I, respectively for *ICAM* and *P-selectin*). These findings suggest that TX attenuates the inflammatory response in the HCE 3D model by modulating key adhesion molecules involved in leukocyte recruitment and epithelial activation (scores in Fig. 5E,J, respectively for *ICAM* and *P-selectin*).

4. Discussion

Oxidative stress and inflammation are mechanisms underlying corneal damage, causing inadequate tear production, excessive evaporation, or an imbalance in tear composition that damages the ocular surface. Several studies show that pathologies such as ocular surface injuries and DED are characterized by the loss of redox homeostasis at both the tear film and conjunctival level, with a marked production of *LPO, MPO*, or *NOS3*, and ROS markers [43]. In this context, nuclear factor erythroid 2-related factor 2 (Nrf2) plays a crucial role as a primary signaling hub regulating the expression of genes involved in antioxidant defense and cellular detoxification. Under physiological conditions, Nrf2 is strictly controlled, but severe oxidative stress requires its activation and nuclear translocation to induce cytoprotective enzymes and neutralize reactive species on the ocular surface [44,45]. Notably, our analysis revealed a significant upregulation of this transcription factor in the TX-treated groups. This finding provides a robust molecular rationale for the parallel increase observed in key downstream cytoprotective enzymes, such as heme oxygenase-1 (*HO-1*), manganese superoxide dismutase (*MnSOD*), and catalase (*CAT*). Importantly, excessive ROS accumulation not only directly damages corneal cells, but also promotes the activation of inflammatory signaling pathways, leading to the release of pro-inflammatory cytokines and the recruitment of immune cells that further exacerbate tissue injury [46,47]. Therefore, the loss of antioxidant defense homeostasis seems to be a key factor in the pathophysiology of these conditions, which also triggers the activation of the inflammatory cascade in the tissues of the ocular surface. In this context, our results indicated the activation of the inflammatory cascade through the increased expression of key pro-inflammatory cytokines, including *IL-8*, *IL-6*, and *IL-1β*. Crucially, to elucidate the upstream molecular orchestrators driving this inflammatory response, we investigated the NF-κB signaling. The nuclear factor kappa B (NF-κB) is a master transcription factor that translocates to the nucleus to promote the transcription of multiple pro-inflammatory genes [48]. In our model, H_2O_2 exposure triggered a marked upregulation of NF-κB, which directly correlates with the massive release of downstream cytokines, which was remarkably restored back toward baseline conditions by TX treatment. These

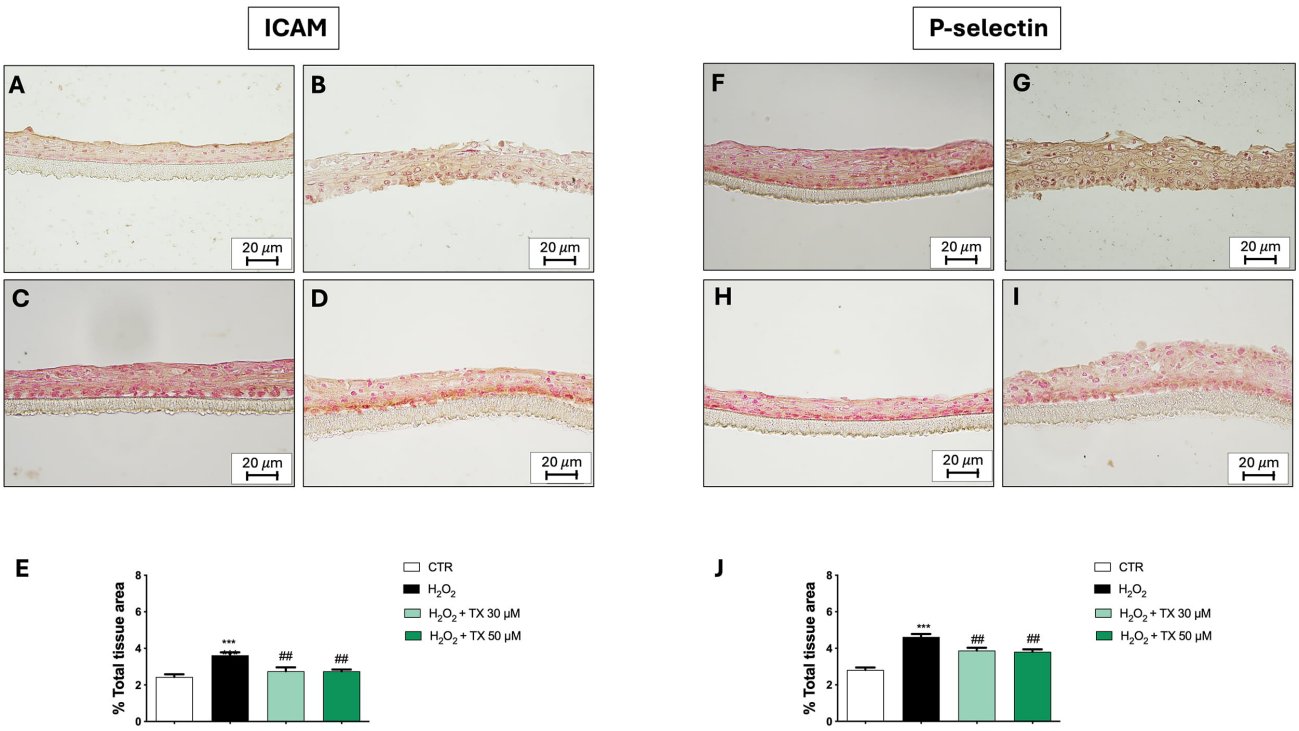

Fig. 5. Effect of troxerutin on *ICAM* and *P-selectin* immunopositivity. H_2O_2 treatment increased *ICAM-1* and *P-selectin* expression, indicating epithelial inflammatory activation, while TX treatment (30 and 50 µM) significantly reduced the immunopositivity of both markers. (A,F) CTR group. (B,G) H_2O_2 Group. (C,H) H_2O_2 + TX 30 µM Group. (D,I) H_2O_2 + TX 50 µM Group. (E,J) The percentage of total tissue area. Values are means ± SEM. *** $p < 0.001$ vs group CTR; ## $p < 0.01$ vs H_2O_2 group. One-way ANOVA test followed by Bonferroni post hoc test for multiple comparisons was used. *ICAM-1*, intercellular adhesion molecule-1. Scale bar: 20 µm.

mediators are known to play a central role in ocular surface inflammation by amplifying leukocyte activation, promoting the expression of adhesion molecules, and perpetuating epithelial tissue damage. In particular, *IL-8* and *IL-1β* are strongly associated with oxidative stress-mediated inflammatory responses and are able to induce the upregulation of *ICAM-1* [49,50] and selectins on epithelial and endothelial cells, thereby facilitating inflammatory cell adhesion and infiltration. Moreover, *IL-6* contributes to the maintenance of chronic inflammatory conditions and has been implicated in the disruption of corneal epithelial homeostasis [51]. Therefore, the increased levels of these cytokines observed in our model further support the existence of a close interplay between oxidative stress and inflammatory activation in corneal injury. Currently, several preventive and therapeutic approaches using antioxidant compounds have been evaluated in several studies [52]. Studies in mouse models of DED have shown that topical application of quercetin reduced the expression of inflammatory markers, including *MMP-2*, *MMP-9*, *ICAM-1*, and *VCAM-1* in the tear gland, protecting the ocular surface and improving corneal integrity [53,54,55]. Similarly, green tea catechins have also demonstrated antioxidant activity by effectively preventing H_2O_2-mediated oxidation of human cataract γ-crystalline and by inhibiting different types of IL-1-induced cytokines or hyperosmolarity in corneal epithelial cells *in vitro* [56,57]. In line with this evidence, our results showed that the antioxidant effect of TX was able to protect corneal tissue from oxidative damage, reducing *MMP-9* release and moderating the disorganization of corneal tissue architecture. The membrane proteins *ICAM-1* and *P-selectin* may play an important role in the cell-mediated immune response and inflammation associated with corneal damage [58]. Recently, *ICAM-1* inhibition with specific antagonists and blocking both *P-selectin* and *e-selectin* represent a promising approach in reducing intraocular inflammation [59,60]. Consistent with the literature, our results show that TX was able to reduce *ICAM-1* and *P-selectin*-mediated immune cell recruitment by promoting the reduction of the inflammatory response induced by oxidative damage [61]. Importantly, persistent inflammatory activation and oxidative stress are known to impair epithelial barrier integrity by disrupting tight junction proteins, ultimately compromising corneal permeability and tissue homeostasis [62]. Two important components of the corneal epithelium that regulate its barrier function are *Occludin* and *ZO-1* tight junctions [63]. Some promising treatments for corneal damage have demonstrated the ability to promote the reconstruction of the corneal epithelial barrier following hyperosmotic stress damage in HCE-2 cells [64]. In line with these findings, TX was able to restore the integrity of the epithelial barrier of corneal tissue through the overexpression of the tight junc-

tions *ZO-1* and *Occludin*, an effect that, added to the antioxidant and anti-inflammatory activity, supports its potential use in the treatment of oxidative stress-related corneal disorders.

5. Limitations and Future Perspectives

Although anti-inflammatory and barrier-protective effects of TX were observed, no direct functional assessment of epithelial permeability was performed; this will be addressed in future studies through dedicated permeability assays to better characterize barrier integrity (e.g., transepithelial electrical resistance [TEER] or fluorescein permeability assays). In addition, the study was conducted exclusively using the SkinEthic™ HCE 3D model, which represents an advanced and highly relevant *in vitro* system that closely mimics the structure and physiology of the human corneal epithelium, making it particularly suitable for ocular surface investigations. Nevertheless, the absence of *in vivo* validation limits the direct translational applicability of the findings; therefore, future studies will include *in vivo* experiments to validate the protective effects of TX under physiological conditions. Overall, these additional approaches will help strengthen and extend the present findings.

6. Conclusions

This study highlighted the antioxidant and anti-inflammatory properties of TX and its ability to mitigate oxidative damage, reduce inflammatory cell recruitment, and restore the integrity of the corneal epithelial barrier after oxidative damage. Although further investigations are needed to validate its efficacy and to optimize its application in the treatment of oxidative stress-related corneal disorders, these findings support the beneficial effect of TX as an adjuvant in the management of such debilitating conditions.

Availability of Data and Materials

The datasets used and analyzed during the current study are available from the corresponding author on reasonable request.

Author Contributions

RB: Methodology, Writing- Original draft preparation, AF: Writing- Reviewing and Editing, and performed the research, NP: Methodology, GC: Software, Validation, ML: Software, Data curation, EE: Supervision and participated in designing the research study, IP: Conceptualization, Visualization. All authors contributed to editorial changes in the manuscript. All authors read and approved the final manuscript. All authors have participated sufficiently in the work and agreed to be accountable for all aspects of the work.

Ethics Approval and Consent to Participate

Not applicable.

Acknowledgment

Graphical abstract was created with Biorender.com. Basilotta, R. (2026) https://BioRender.com/sc2b1kp.

Funding

This research received no external funding.

Conflicts of Interest

The authors declare no conflicts of interest. Given her role as the Guest Editor, Alessia Filippone had no involvement in the peer-review of this article and has no access to information regarding its peer review. Full responsibility for the editorial process for this article was delegated to Sarah D. Atkinson.

References

[1] Bazeer S, Jansonius N, Snieder H, Hammond C, Vehof J. The relationship between occupation and dry eye. The Ocular Surface. 2019; 17: 484–490. https://doi.org/10.1016/j.jtos.2019.04.004

[2] Cejka C, Cejkova J. Oxidative stress to the cornea, changes in corneal optical properties, and advances in treatment of corneal oxidative injuries. Oxidative Medicine and Cellular Longevity. 2015; 2015: 591530. https://doi.org/10.1155/2015/591530

[3] Nelson JD, Craig JP, Akpek EK, Azar DT, Belmonte C, Bron AJ, et al. TFOS DEWS II Introduction. The Ocular Surface. 2017; 15: 269–275. https://doi.org/10.1016/j.jtos.2017.05.005

[4] Kaluzhny Y, Kinuthia MW, Lapointe AM, Truong T, Klausner M, Hayden P. Oxidative stress in corneal injuries of different origin: Utilization of 3D human corneal epithelial tissue model. Experimental Eye Research. 2020; 190: 107867. https://doi.org/10.1016/j.exer.2019.107867

[5] Batliwala S, Xavier C, Liu Y, Wu H, Pang IH. Involvement of Nrf2 in Ocular Diseases. Oxidative Medicine and Cellular Longevity. 2017; 2017: 1703810. https://doi.org/10.1155/2017/1703810

[6] Dogru M, Kojima T, Simsek C, Tsubota K. Potential Role of Oxidative Stress in Ocular Surface Inflammation and Dry Eye Disease. Investigative Ophthalmology & Visual Science. 2018; 59: DES163–DES168. https://doi.org/10.1167/iovs.17-23402

[7] Shimazaki J. Definition and Diagnostic Criteria of Dry Eye Disease: Historical Overview and Future Directions. Investigative Ophthalmology & Visual Science. 2018; 59: DES7–DES12. https://doi.org/10.1167/iovs.17-23475

[8] Drew VJ, Tseng CL, Seghatchian J, Burnouf T. Reflections on Dry Eye Syndrome Treatment: Therapeutic Role of Blood Products. Frontiers in Medicine. 2018; 5: 33. https://doi.org/10.3389/fmed.2018.00033

[9] Li B, Sheng M, Li J, Yan G, Lin A, Li M, et al. Tear proteomic analysis of Sjögren syndrome patients with dry eye syndrome by two-dimensional-nano-liquid chromatography coupled with tandem mass spectrometry. Scientific Reports. 2014; 4: 5772. https://doi.org/10.1038/srep05772

[10] Navel V, Sapin V, Henrioux F, Blanchon L, Labbé A, Chiambaretta F, et al. Oxidative and antioxidative stress markers in dry eye disease: A systematic review and meta-analysis. Acta Ophthalmologica. 2022; 100: 45–57. https://doi.org/10.1111/aos.14892

[11] Ray PD, Huang BW, Tsuji Y. Reactive oxygen species (ROS)

homeostasis and redox regulation in cellular signaling. Cellular Signalling. 2012; 24: 981–990. https://doi.org/10.1016/j.cellsig.2012.01.008

[12] Choi JH, Li Y, Kim SH, Jin R, Kim YH, Choi W, et al. The influences of smartphone use on the status of the tear film and ocular surface. PLoS ONE. 2018; 13: e0206541. https://doi.org/10.1371/journal.pone.0206541

[13] Wakamatsu TH, Dogru M, Matsumoto Y, Kojima T, Kaido M, Ibrahim OMA, et al. Evaluation of lipid oxidative stress status in Sjögren syndrome patients. Investigative Ophthalmology & Visual Science. 2013; 54: 201–210. https://doi.org/10.1167/iovs.12-10325

[14] Kolesnikov A, Shchulkin A, Barenina O, Konopleva V. Local and systemic antioxidant status in experimental purulent corneal ulcer. Kazan medical journal. 2013; 94: 571–575. https://doi.org/10.17816/KMJ1974

[15] Thulasi P, Djalilian AR. Update in Current Diagnostics and Therapeutics of Dry Eye Disease. Ophthalmology. 2017; 124: S27–S33. https://doi.org/10.1016/j.ophtha.2017.07.022

[16] Dai Y, Zhang J, Xiang J, Li Y, Wu D, Xu J. Calcitriol inhibits ROS-NLRP3-IL-1β signaling axis via activation of Nrf2-antioxidant signaling in hyperosmotic stress stimulated human corneal epithelial cells. Redox Biology. 2019; 21: 101093. https://doi.org/10.1016/j.redox.2018.101093

[17] Li S, Lu Z, Huang Y, Wang Y, Jin Q, Shentu X, et al. Anti-Oxidative and Anti-Inflammatory Micelles: Break the Dry Eye Vicious Cycle. Advanced Science (Weinheim, Baden-Wurttemberg, Germany). 2022; 9: e2200435. https://doi.org/10.1002/advs.202200435

[18] Zhang Y, An Y, He X, Zhang D, He W. Esculetin protects human corneal epithelial cells from oxidative stress through Nrf-2 signaling pathway. Experimental Eye Research. 2021; 202: 108360. https://doi.org/10.1016/j.exer.2020.108360

[19] Li J, Ruzhi Deng, Hua X, Zhang L, Lu F, Coursey TG, et al. Blueberry Component Pterostilbene Protects Corneal Epithelial Cells from Inflammation via Anti-oxidative Pathway. Scientific Reports. 2016; 6: 19408. https://doi.org/10.1038/srep19408

[20] Panat NA, Maurya DK, Ghaskadbi SS, Sandur SK. Troxerutin, a plant flavonoid, protects cells against oxidative stress-induced cell death through radical scavenging mechanism. Food Chemistry. 2016; 194: 32–45. https://doi.org/10.1016/j.foodchem.2015.07.078

[21] Dehnamaki F, Karimi A, Pilevarian AA, Fatemi I, Hakimizadeh E, Kaeidi A, et al. Treatment with troxerutin protects against cisplatin-induced kidney injury in mice. Acta Chirurgica Belgica. 2019; 119: 31–37. https://doi.org/10.1080/00015458.2018.1455418

[22] Thomas NS, George K, Arivalagan S, Mani V, Siddique AI, Namasivayam N. The in vivo antineoplastic and therapeutic efficacy of troxerutin on rat preneoplastic liver: biochemical, histological and cellular aspects. European Journal of Nutrition. 2017; 56: 2353–2366. https://doi.org/10.1007/s00394-016-1275-0

[23] Lu J, Wu DM, Zheng YL, Hu B, Cheng W, Zhang ZF, et al. Troxerutin counteracts domoic acid-induced memory deficits in mice by inhibiting CCAAT/enhancer binding protein β-mediated inflammatory response and oxidative stress. Journal of Immunology (Baltimore, Md.: 1950). 2013; 190: 3466–3479. https://doi.org/10.4049/jimmunol.1202862

[24] Ping X, Junqing J, Junfeng J, Enjin J. Radioprotective effects of troxerutin against gamma irradiation in mice liver. International Journal of Radiation Biology. 2012; 88: 607–612. https://doi.org/10.3109/09553002.2012.692494

[25] Baluchnejadmojarad T, Jamali-Raeufy N, Zabihnejad S, Rabiee N, Roghani M. Troxerutin exerts neuroprotection in 6-hydroxydopamine lesion rat model of Parkinson's disease: Possible involvement of PI3K/ERβ signaling. European Journal of Pharmacology. 2017; 801: 72–78. https://doi.org/10.1016/j.ejphar.2017.03.002

[26] Yu Y, Zheng G. Troxerutin protects against diabetic cardiomyopathy through NF-κB/AKT/IRS1 in a rat model of type 2 diabetes. Molecular Medicine Reports. 2017; 15: 3473–3478. https://doi.org/10.3892/mmr.2017.6456

[27] Malinska H, Hüttl M, Oliyarnyk O, Markova I, Poruba M, Racova Z, et al. Beneficial effects of troxerutin on metabolic disorders in non-obese model of metabolic syndrome. PLoS ONE. 2019; 14: e0220377. https://doi.org/10.1371/journal.pone.0220377

[28] Arab HH, Abd El-Aal SA, Eid AH, Arafa ESA, Mahmoud AM, Ashour AM. Targeting inflammation, autophagy, and apoptosis by troxerutin attenuates methotrexate-induced renal injury in rats. International Immunopharmacology. 2022; 103: 108284. https://doi.org/10.1016/j.intimp.2021.108284

[29] Bova V, Basilotta R, Casili G, Lanza M, Filippone A, Campolo M, et al. The Protective Role of Troxerutin (Trox) in Counteracting Anaplastic Thyroid Carcinoma (ATC) Progression. Biomedicines. 2024; 12: 1755. https://doi.org/10.3390/biomedicines12081755

[30] Subastri A, Suyavaran A, Preedia Babu E, Nithyananthan S, Barathidasan R, Thirunavukkarasu C. Troxerutin with copper generates oxidative stress in cancer cells: Its possible chemotherapeutic mechanism against hepatocellular carcinoma. Journal of Cellular Physiology. 2018; 233: 1775–1790. https://doi.org/10.1002/jcp.26061

[31] Fahmideh F, Marchesi N, Campagnoli LIM, Landini L, Caramella C, Barbieri A, et al. Effect of troxerutin in counteracting hyperglycemia-induced VEGF upregulation in endothelial cells: a new option to target early stages of diabetic retinopathy? Frontiers in Pharmacology. 2022; 13: 951833. https://doi.org/10.3389/fphar.2022.951833

[32] Fahmideh F. Targeting early stages of diabetic retinopathy: the modulation of VEGF via PKCβII/HuR cascade [PhD thesis]. University of Pavia. 2022.

[33] Alépée N, Leblanc V, Grandidier MH, Teluob S, Tagliati V, Adriaens E, et al. Development of the SkinEthic HCE Time-to-Toxicity test method for identifying liquid chemicals not requiring classification and labelling and liquids inducing serious eye damage and eye irritation. Toxicology in Vitro: an International Journal Published in Association with BIBRA. 2020; 69: 104960. https://doi.org/10.1016/j.tiv.2020.104960

[34] Alépée N, Grandidier MH, Teluob S, Amaral F, Caviola E, De Servi B, et al. Validation of the SkinEthic HCE Time-to-Toxicity test method for eye hazard classification of chemicals according to UN GHS. Toxicology in Vitro: an International Journal Published in Association with BIBRA. 2022; 80: 105319. https://doi.org/10.1016/j.tiv.2022.105319

[35] Filippone A, Lanza M, Campolo M, Casili G, Paterniti I, Cuzzocrea S, et al. The Anti-Inflammatory and Antioxidant Effects of Sodium Propionate. International Journal of Molecular Sciences. 2020; 21: 3026. https://doi.org/10.3390/ijms21083026

[36] Xu Y, Wang S, Miao Q, Jin K, Lou L, Ye X, et al. Protective Role of Hinokitiol Against H_2O_2-Induced Injury in Human Corneal Epithelium. Current Eye Research. 2017; 42: 47–53. https://doi.org/10.3109/02713683.2016.1151530

[37] Abbate I, Zappulla C, Santonocito M, Viola S, La Rosa LR, De Pasquale G, et al. Preclinical study of a new matrix to help the ocular surface in dry eye disease. Experimental Eye Research. 2022; 222: 109168. https://doi.org/10.1016/j.exer.2022.109168

[38] Paterniti I, Cordaro M, Campolo M, Siracusa R, Cornelius C, Navarra M, et al. Neuroprotection by association of palmitoylethanolamide with luteolin in experimental Alzheimer's disease models: the control of neuroinflammation. CNS & Neu-

rological Disorders Drug Targets. 2014; 13: 1530–1541. https://doi.org/10.2174/1871527313666140806124322

[39] Khoh-Reiter S, Jessen BA. Evaluation of the cytotoxic effects of ophthalmic solutions containing benzalkonium chloride on corneal epithelium using an organotypic 3-D model. BMC Ophthalmology. 2009; 9: 5. https://doi.org/10.1186/1471-2415-9-5

[40] Paterniti I, Impellizzeri D, Cordaro M, Siracusa R, Bisignano C, Gugliandolo E, et al. The Anti-Inflammatory and Antioxidant Potential of Pistachios (Pistacia vera L.) In Vitro and In Vivo. Nutrients. 2017; 9: 915. https://doi.org/10.3390/nu9080915

[41] Scuderi SA, Cucinotta L, Filippone A, Lanza M, Campolo M, Paterniti I, et al. Effect of Melatonin on Psoriatic Phenotype in Human Reconstructed Skin Model. Biomedicines. 2022; 10: 752. https://doi.org/10.3390/biomedicines10040752

[42] Campbell M, Cassidy PS, O'Callaghan J, Crosbie DE, Humphries P. Manipulating ocular endothelial tight junctions: Applications in treatment of retinal disease pathology and ocular hypertension. Progress in Retinal and Eye Research. 2018; 62: 120–133. https://doi.org/10.1016/j.preteyeres.2017.09.003

[43] Vehof J, Utheim TP, Bootsma H, Hammond CJ. Advances, limitations and future perspectives in the diagnosis and management of dry eye in Sjögren's syndrome. Clinical and Experimental Rheumatology. 2020; 38: S301–S309.

[44] Liu XF, Zhou DD, Xie T, Malik TH, Lu CB, Li HJ, et al. Nrf2, a Potential Therapeutic Target against Oxidative Stress in Corneal Diseases. Oxidative Medicine and Cellular Longevity. 2017; 2017: 2326178. https://doi.org/10.1155/2017/2326178

[45] Jiang XY, Guo QQ, Wang SS, Guo R, Zou Y, Liu JW, et al. DNA damage response pathway regulates Nrf2 in response to oxidative stress. Science Advances. 2025; 11: eadu9555. https://doi.org/10.1126/sciadv.adu9555

[46] Zhang M, Zhang R, Zhao X, Ma Z, Xin J, Xu S, et al. The role of oxidative stress in the pathogenesis of ocular diseases: an overview. Molecular Biology Reports. 2024; 51: 454. https://doi.org/10.1007/s11033-024-09425-5

[47] Ahmad A, Ahsan H. Biomarkers of inflammation and oxidative stress in ophthalmic disorders. Journal of Immunoassay & Immunochemistry. 2020; 41: 257–271. https://doi.org/10.1080/15321819.2020.1726774

[48] Rothwarf DM, Karin M. The NF-kappa B activation pathway: a paradigm in information transfer from membrane to nucleus. Science's STKE: Signal Transduction Knowledge Environment. 1999; 1999: RE1. https://doi.org/10.1126/stke.1999.5.re1

[49] Wu X, Chen X, Ma Y, Lin X, Yu X, He S, et al. Analysis of tear inflammatory molecules and clinical correlations in evaporative dry eye disease caused by meibomian gland dysfunction. International Ophthalmology. 2020; 40: 3049–3058. https://doi.org/10.1007/s10792-020-01489-z

[50] Dammak A, Huete-Toral F, Carpena-Torres C, Martin-Gil A, Pastrana C, Carracedo G. From Oxidative Stress to Inflammation in the Posterior Ocular Diseases: Diagnosis and Treatment. Pharmaceutics. 2021; 13: 1376. https://doi.org/10.3390/pharmaceutics13091376

[51] Sugaya S, Sakimoto T, Shoji J, Sawa M. Regulation of soluble interleukin-6 (IL-6) receptor release from corneal epithelial cells and its role in the ocular surface. Japanese Journal of Ophthalmology. 2011; 55: 277–282. https://doi.org/10.1007/s10384-011-0002-x

[52] Rodella U, Honisch C, Gatto C, Ruzza P, D'Amato Tóthová J. Antioxidant Nutraceutical Strategies in the Prevention of Oxidative Stress Related Eye Diseases. Nutrients. 2023; 15: 2283. https://doi.org/10.3390/nu15102283

[53] Panche AN, Diwan AD, Chandra SR. Flavonoids: an overview. Journal of Nutritional Science. 2016; 5: e47. https://doi.org/10.1017/jns.2016.41

[54] Oh HN, Kim CE, Lee JH, Yang JW. Effects of Quercetin in a Mouse Model of Experimental Dry Eye. Cornea. 2015; 34: 1130–1136. https://doi.org/10.1097/ICO.0000000000000543

[55] Cheng SC, Wu YH, Huang WC, Pang JHS, Huang TH, Cheng CY. Anti-inflammatory property of quercetin through down-regulation of ICAM-1 and MMP-9 in TNF-α-activated retinal pigment epithelial cells. Cytokine. 2019; 116: 48–60. https://doi.org/10.1016/j.cyto.2019.01.001

[56] Cavet ME, Harrington KL, Vollmer TR, Ward KW, Zhang JZ. Anti-inflammatory and anti-oxidative effects of the green tea polyphenol epigallocatechin gallate in human corneal epithelial cells. Molecular Vision. 2011; 17: 533–542.

[57] Lee HS, Chauhan SK, Okanobo A, Nallasamy N, Dana R. Therapeutic efficacy of topical epigallocatechin gallate in murine dry eye. Cornea. 2011; 30: 1465–1472. https://doi.org/10.1097/ICO.0b013e31821c9b5a

[58] Pflugfelder SC, Stern M, Zhang S, Shojaei A. LFA-1/ICAM-1 Interaction as a Therapeutic Target in Dry Eye Disease. Journal of Ocular Pharmacology and Therapeutics: the Official Journal of the Association for Ocular Pharmacology and Therapeutics. 2017; 33: 5–12. https://doi.org/10.1089/jop.2016.0105

[59] Heidary F, Ardestani SK, Ghasemi H, Javadi MA, Mahmoudi M, Yaraee R, et al. Alteration in serum levels of ICAM-1 and P-, E- and L-selectins in seriously eye-injured long-term following sulfur-mustard exposure. International Immunopharmacology. 2019; 76: 105820. https://doi.org/10.1016/j.intimp.2019.105820

[60] Paton DM. Lifitegrast: First LFA-1/ICAM-1 antagonist for treatment of dry eye disease. Drugs of Today (Barcelona, Spain: 1998). 2016; 52: 485–493. https://doi.org/10.1358/dot.2016.52.9.2542066

[61] Pflugfelder SC, de Paiva CS. The Pathophysiology of Dry Eye Disease: What We Know and Future Directions for Research. Ophthalmology. 2017; 124: S4–S13. https://doi.org/10.1016/j.ophtha.2017.07.010

[62] Anupama C, Shettar A, Ranganath SH, Srinivas SP. Experimental Oxidative Stress Breaks Down the Barrier Function of the Corneal Endothelium. Journal of Ocular Pharmacology and Therapeutics: the Official Journal of the Association for Ocular Pharmacology and Therapeutics. 2023; 39: 70–79. https://doi.org/10.1089/jop.2022.0093

[63] Tanaka H, Fukuda K, Ishida W, Harada Y, Sumi T, Fukushima A. Rebamipide increases barrier function and attenuates TNFα-induced barrier disruption and cytokine expression in human corneal epithelial cells. The British Journal of Ophthalmology. 2013; 97: 912–916. https://doi.org/10.1136/bjophthalmol-2012-302868

[64] Dong Y, Ding YY, Gao WP. Puerarin alleviates hyperosmotic stress-induced oxidative stress, inflammation, apoptosis and barrier damage of human corneal epithelial cells by targeting SIRT1/NLRP3 signaling. Toxicology in Vitro: an International Journal Published in Association with BIBRA. 2024; 94: 105722. https://doi.org/10.1016/j.tiv.2023.105722